STUDY ON THE PLASTIC DEFORMATION DURING CLEAVAGE ON MgO SINGLE CRYSTALS

FUTAGAMI, Koji
Research Institute for Applied Mechanics, Kyushu University : Associate Professor

AKASHI, Yoshito
Research Institute for Applied Mechanics, Kyushu University : Research Associate

https://doi.org/10.5109/7172625

出版情報：Reports of Research Institute for Applied Mechanics. 20 (66), pp.21-35, 1973. 九州大学応用力学研究所
バージョン：
権利関係：

Reports of Research Institute for Applied Mechanics
Vol. XX, No. 66, 1973

STUDY ON THE PLASTIC DEFORMATION DURING CLEAVAGE ON MgO SINGLE CRYSTALS†

By Kōji FUTAGAMI* and Yoshito AKASHI**

MgO single crystals with $\sim 10^6$ dislocations/cm^2 and $\sim$ 1mm^2 sub-grains are cleaved at room temperature and observed mainly by limited projection topography. The fresh dislocations nucleated near the cleaved surface are found at large cleavage step of $\sim 30\mu$ in height. They are straight edge dislocations in the $\langle 100 \rangle$ direction with separation distance 14 μ, average length 0.3 mm and penetration depth from the surface$\sim$10 μ. The configu ration of these dislocations supports the mechanism of fracture proposed by Gilman and Kitajima, that the movement of these nucleated dislocations contributes to the plastic deformation near the fracture surface during the propagation of cleavage crack. On the basis of the theory developed by Burns *et al.*, the increment in the effective surface energy during cleavage is estimated to be several percent of the intrinsic one, which is much smaller than that measured on LiF.

1. Introduction

The discrimination between the brittle mode and ductile mode in crystal fracture is predicted theoretically from the relation between the shear stress and the fracture stress, breaking an atom-to-atom bond, in an ideally perfect crystal. However, phenomena of fracture are not the uniform deformation of crystal, but are the propagation and the development of fracture surface which appears locally. When we discuss the mechanism of fracture, we have to consider not only the characteristics inherent to a crystal but the contribution of lattice defects to plastic deformation. To elucidate the mechanism of fracture, the study of this plastic work during the nucleation and propagation of fracture is important. It is necessary to study experimentally effects of various factors concerning to this mechanism one by one. For it is impossible to estimate the plastic work in localized part theoretically.

For this purpose, cleavage fracture is studied in this report, because this is usually accompanied by a little plastic deformation and is relatively reproduci-

† The essential part of this paper was reported in the Japanese Journal of Applied Physics. [Vol. 11 (1972) pp. 1265-1272]
* Associate Professor, Research Institute for Applied Mechanics, Kyushu University.
** Research Associate, Research Institute for Applied Mechanics, Kyushu University.

ble. As one of the typical specimens, MgO single crystal is taken. Crystal structure of MgO is of the sodium chloride, and it is relatively simple to elucidate the mechanism of fracture. Besides it has some nature of covalent crystal and is not an ionic crystal in a pure sense. The results will give some clues to understand the superior properties of ceramic materials as follows. They have high melting point, high acid resistance and relatively high strength at high temperatures.

So far much have been studied to clarify the mechanical properties of MgO,[1-6] but little systematic studies have been made on the plastic deformation which appears on the fracture surface during cleavage. While, on ionic crystals such as semi-ductile LiF,[7-14] many studies on this problem have been made. In the theoretical investigation to explain the brittleness of crystals, Tyson[15] and Cottrell *et al.*[16] calculated the stress required to break an atom-to-atom bond in ideally perfect crystals and gave the characteristic values which show the brittleness of crystals.

In this report, the plastic deformation which occurs on the cleavage surface of MgO single crystals cleaved at room temperature are mainly observed by the X-ray diffraction topography. Comparison are made between the results on MgO and LiF. By substituting the present results into theoretical equations derived for LiF by Burns *et al.*,[12,13] the increment in the effective surface energy caused by plastic deformation is estimated.

2. Experimental Procedures

MgO single crystals of specified spectroscopic grade purchased from Norton Chemical Company were used. They were about $7 \times 7 \times 7$ mm^3 and have grown-in dislocation density $\sim 10^6/\mathrm{cm}^2$ within sub-grains of about 1 mm^2. MgO single crystals can be cleaved well along the {100} planes even at relatively high temperatures. The blocks were cleaved into specimens of 1 mm thickness at room temperature by a chisel with a sharp knife edge. The average speed of cleavage cracks generated by a blow on the chisel should be very high.

The slip system of MgO single crystals is $\{110\}\langle 1\bar{1}0\rangle$, where one slip plane corresponds to one slip direction. Two groups of slip bands may be seen on {100} planes as shown in Fig. 1. One of them consists of four 45° bands or screw bands, which make an angle of 45° with {100} planes and the other two 90° bands or edge bands, which make an angle of 90°. When the chisel is placed on the $(0\bar{1}0)$ with direction of the knife edge along the [001] and an impact is given to it in the [010] direction, the specimen is cleaved on the (100) plane. In such cleavage, the active slip planes are exclusively the 45° bands, as discussed in section 4.2.

X-ray diffraction topography, the limited projection type[17-19] was mainly used. Fig. 2 shows a shematic diagram of this method. To take the limited projection topographs, the limiting slit is inserted in a position between the specimen and the plate. By the setting position *LS* 1 in Fig. 2, we obtain the topographs of limited portion inside the crystal lying within the layer of *ABCD*.

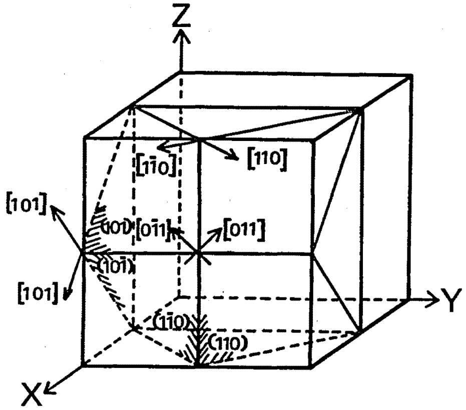

Fig. 1 The crystal orientation and the slip system of MgO single crystal.

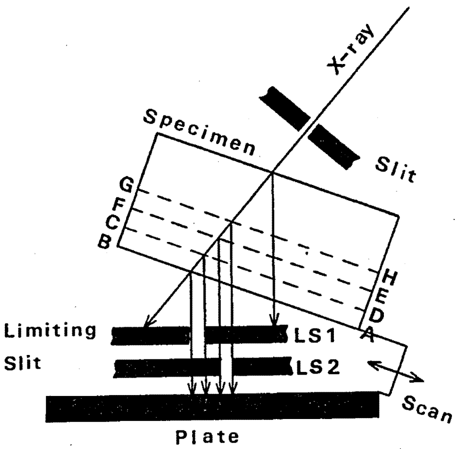

Fig. 2 Schematic diagram of experimental arrangement for the limited projection topography. Limited portion of the specimen parallel to scanning direction is taken using limiting slit whose position and width are variable.

And by *LS* 2 that within *EFGH*.

To resolve the individual dislocations in a crystal with $10^6/cm^2$ is the limit for ordinary X-ray diffraction topography, and studies have been almost made by transmission electron microscope or etch pit technique. But the limited projection topography makes it possible to observe clearly individual dislocations in the crystals even with 10^6 dislocations/cm^2. A typical example is shown in Photo 1. Besides the three-dimensional configuration of lattice defects can be determined taking a series of limited projection topographs with a change of setting position of the limiting slit.

The (010), (001), (011) and $(0\bar{1}1)$ diffraction planes which are perpendicular to the cleaved surface were taken. Mokα_1 radiation was used under the operating condition of 45kV and 0.7 mA. The effective focal size of X-ray source was $50\mu \times 50\mu$. In this experimental condition, μt was about 1 where μ is linear absorption coefficient of MgO and t is its thickness. Sakura nuclear plates El (emulsion thickness 50μ) were used and the exposure time was 4 hours/mm. Stereo topographs were also taken. Detailed observations of river lines and steps on cleaved surfaces were made with optical and interference microscope, respectively, to determine the direction of crack propagation and the height of cleavage steps. Etch pit technique was also used. Specimens were etched with hot ortho phosphoric acid for 8 sec and 15 sec and with a solution consisting of H_2SO_4 and NH_4Cl (ratio 1 : 1) for 1.5 min and 5 min. After being washed and dried with methyl alchohol, they were observed by optical microscope.

3. Experimental Results

A typical limited projection topograph of MgO single crystal cleaved at room temperature is shown in Photo 2. This was taken with diffraction vector, $\boldsymbol{g}=[001]$ and the width of limiting slit 35μ. The effective thickness of the specimen was about 100μ. Photo 2 (b) shows an enlarged view of a part of (a). Parallel dislocations aligned in the [010] direction with separation distance 14μ and average length 0.3 mm are observed near the step, or the black line running downwards obliquely from left to right. The black contrast indicates the enhanced diffraction intensity. In (010) topograph as shown in Photo 3, dislocation lines run in the [001] direction, *i.e.* perpendicular to the direction of the dislocation lines shown in Photo 2. [010] dislocation lines cannot be observed in this topograph. Photo 4 shows a topograph taken with $\boldsymbol{g}=[0\bar{1}1]$. Both the dislocation lines found in Photos 2 and 3, namely, the [010] dislocation lines and the [001] dislocation lines, are observed, though their contrast is inferior to that of Photos 2 and 3, because of diffraction conditions. Similar topographs were obtained when $\boldsymbol{g}=[011]$. In these topographs the density of the fresh dislocations aligned in parallel array is about 1400 cm/cm^2. Their configuration is markedly different from that of grown-in dislocations. Noticeable change of the density of fresh dislocations is not found in the vicinity of subgrain boundaries, where the density of grown-in dislocations is high. Therefore, it is likely that these fresh dislocations were nucleated by concentrated stress at the crack tip during the propagation of cleavage fracture.

A series of topographs were taken with the change of the position of limiting slit in turn and stereo-topographs were also taken by the $(\bar{h}\bar{k}\bar{l})$ and (hkl) pairs in order to determine the three-dimensional structure of fresh dislocations. In that series fresh dislocations can be observed even with a limiting slit too narrow for presenting grown-in dislocations. The depth of fresh dislocations from cleaved surfaces is estimated to be about 10μ. The stereo-topographs also show that those fresh dislocations run parallel to the cleaved surface.

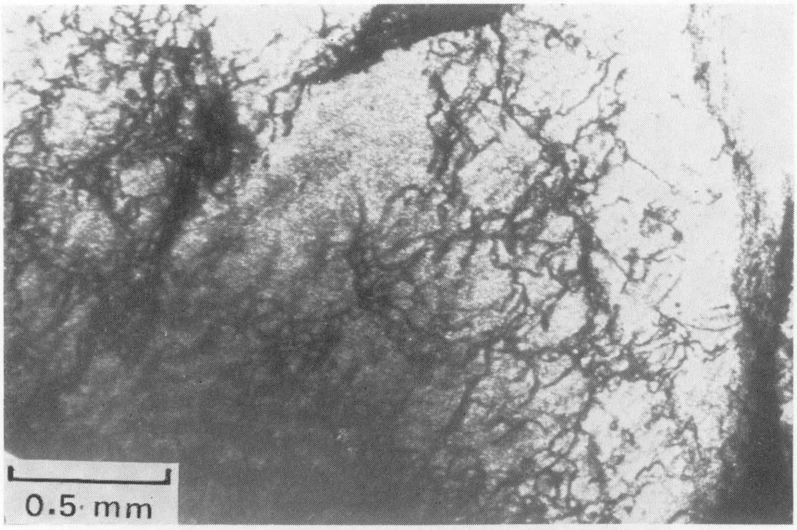

Photo 1 Typical limited projection topograph of MgO with 10^6 dislocations/cm^2 Individual dislocations are clearly observed.

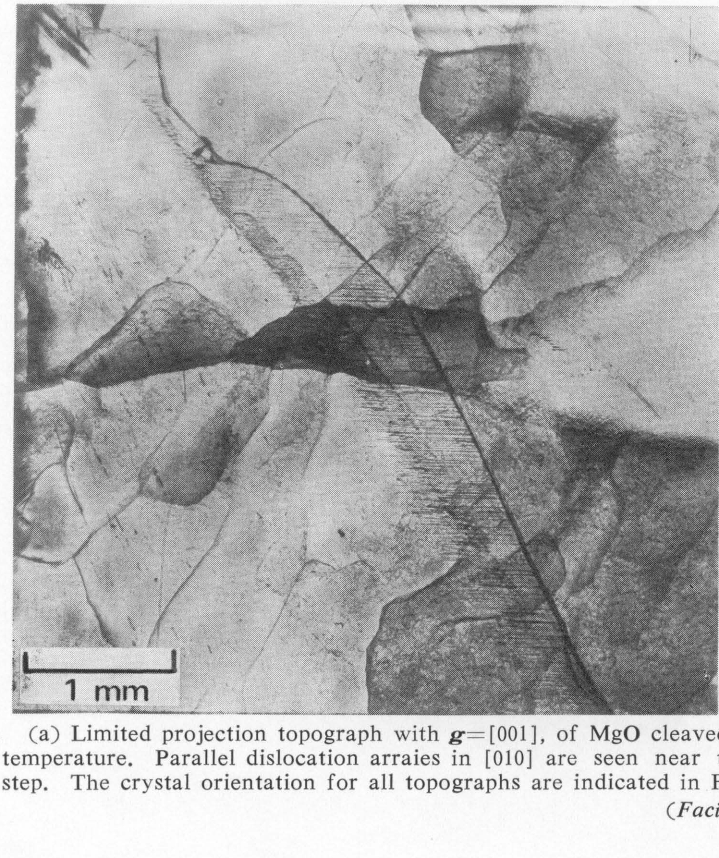

Photo 2 (a) Limited projection topograph with $\boldsymbol{g}=[001]$, of MgO cleaved at room temperature. Parallel dislocation arraies in [010] are seen near the large step. The crystal orientation for all topographs are indicated in Fig. 3.

(*Facing* p. 24)

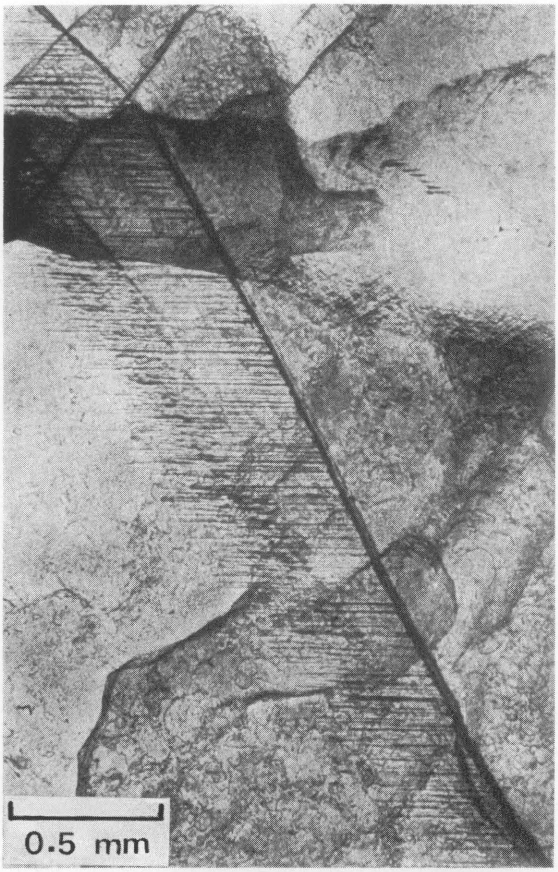

Photo 2 (b)

(b) An enlargement of a part of Photo. 2 (a).

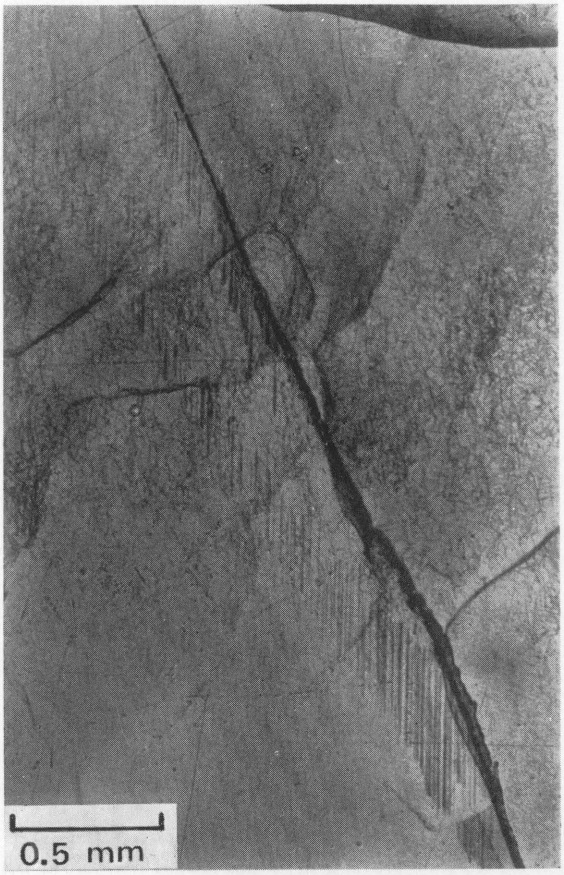

Photo 3 Limited projection topograph with $\boldsymbol{g}=[010]$. Parallel dislocation lines in [001] are observed.

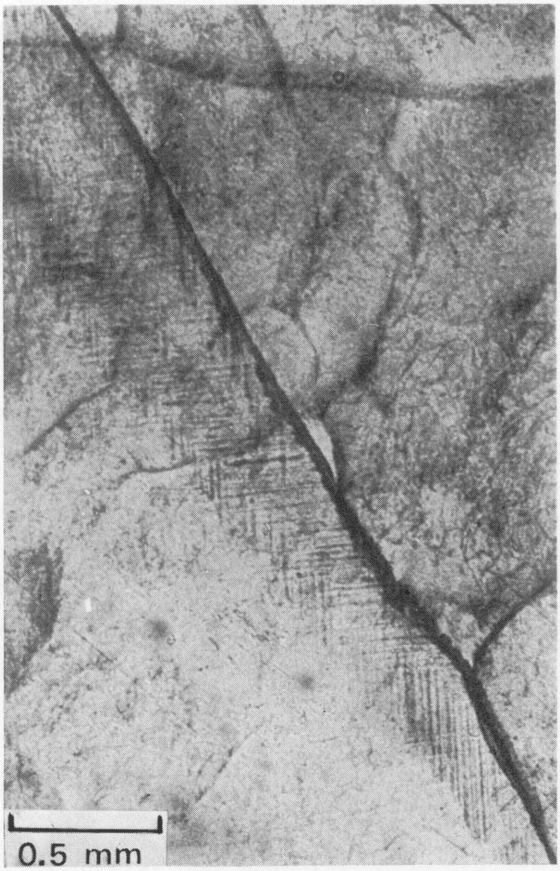

Photo 4 Limited projection topograph with $\boldsymbol{g}=[0\bar{1}1]$. Two groups of dislocation lines. one in [001] and the other in [010], are both observed.

The Burgers vectors of these dislocations were determined from the invisibility criterion; $\boldsymbol{g}\cdot\boldsymbol{b}=0$. The Burgers vector of the [010] dislocation is $[\bar{1}0\bar{1}]$ or $[\bar{1}01]$ and that of the [001] is $[\bar{1}\bar{1}0]$ or $[\bar{1}10]$. Consequently, the fresh dislocations must be edge dislocations.

The cleaved surfaces were examined with an optical microscope for studying the nucleation mechanism of the fresh dislocations. Fig. 3 shows a sketch of a cleaved surface. In this case an impact was of applied in the [010] direction to produce cleavage on the (100) plane. However, the cleavage front did not proceed in [010] direction but deviated toward the $[01\bar{1}]$ direction from the source of initiation *O*. *S* at the center is a large cleavage step about 30μ in height. This step is attributable to the simultaneous propagation of two cleavage cracks initiated from different microscopic origins: one cleaved plane began to extend a little later than the other so that the former thrusted into the latter at the site of the step, as *P*1 or *P*2 where optical interference patterns were observed.

The solid lines in Fig. 3 show river lines lying nearly $[01\bar{1}]$. Photo 5 shows a photograph of river lines through interference microscope. The height of

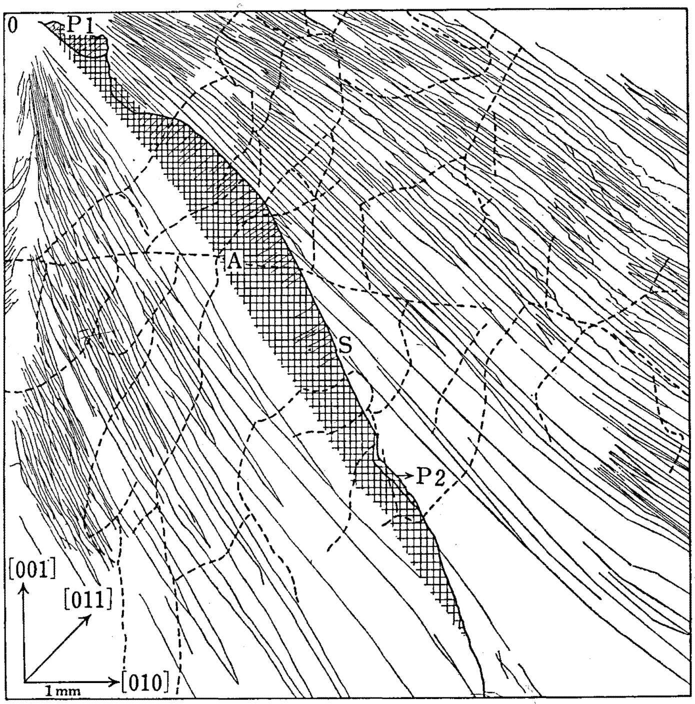

Fig. 3 Sketch of a cleaved surface. Solid lines, closed lines and dotted lines are river lines, fresh dislocations and sub-grain boundaries, respectively. *O*: Origin of fracture. *S*: large step, *A*: region of fresh dislocations, *P1* and *P2*: places presenting optical fringes.

them is measured to be about thousands Å from it. Their density is high outside the region A, where the fresh dislocations detected by topography are shown by the crossed lines. In general fresh dislocations were detected only in these regions like A that were located close to the large step and had smooth surfaces with no or very few river lines running perpendicular to the step. Both the large and small steps seem to have no relations with sub-grain boundaries shown by dotted lines in Fig. 3.

Deformation zones or stoplines owing to low speed of cleavage,[12,14,17] where fresh dislocations often observed in the topographs of cleavage surface of LiF, were not detected in MgO. In MgO, the fresh dislocation so long and deep as to be observed by X-ray diffraction topography are found near the large step and no fresh dislocation are found on the cleaved surfaces where no large steps exist.

On the other hand, dense etch pits were observed at small steps, or river lines, by optical microscope as shown in Photo 6, where no dislocations were observed by X-ray topography. These etch pits may represent small and shallow dislocations which should be nucleated during cleavage fracture.

4. Discussions

4. 1. Estimation for ductility during cleavage

Two kinds of mechanism are known on the plastic deformation of semi-brittle substances that acts in the neighborhood of the fracture surface during the propagation of cleavage crack. Friedel[20] and Tetelman[21] attribute the deformation to the movement of pre-existing dislocations caused by the stress concentration in the neighborhood of cleavage cracks. On the other hand, Gilman[22] and Kitajima[23] attribute the deformation to the movement of newly nucleated dislocation loops during propagation of fracture.

The presence of a long array of dislocations parallel to the {100} plane running in the $\langle 100 \rangle$ direction, as seen in Photos 2–4, supports the latter view. Because the shape of dislocation are straight lines which are characteristic of fresh dislocations rather than grown-in ones, and the observed dislocations have no trace of interference in the regions of high density of grown-in dislocation such as sub-grain boundaries. These facts contradict with Friedel's viewpoint. Besides these facts dissent from the conclusion of Tyson *et al.*[15,16] They calculated the characteristic value β showing the brittleness of a crystal, where $\beta = \sigma_{th}/\tau_{th}$ with the critical normal σ_{th} and the shear stress τ_{th} of a crystal lattice. For ionic and covalent crystals with great ductility, β is nearly equal to 1 and is 5~10 for b. c. c. metals which show ductility at low temperature. And this value is 20~30 for f. c. c. metals which scarcely show ductility. Our calculation shows that β is 1.10 and 1.05 for LiF and MgO respectively. This indicates that the brittleness of these crystals is very large and that the plastic work is very small in dynamic cleavage. It is hard, then, for dislocations to be introduced. On the contrary to this prediction, the experimental results

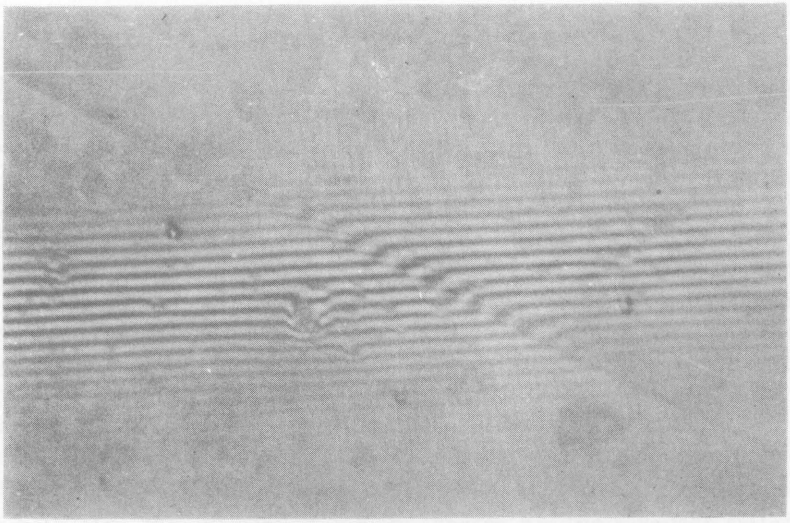

Photo 5 Interference micrograph of river lines. (×1000). The height of a small step of river line is measured to be about thousands Å.

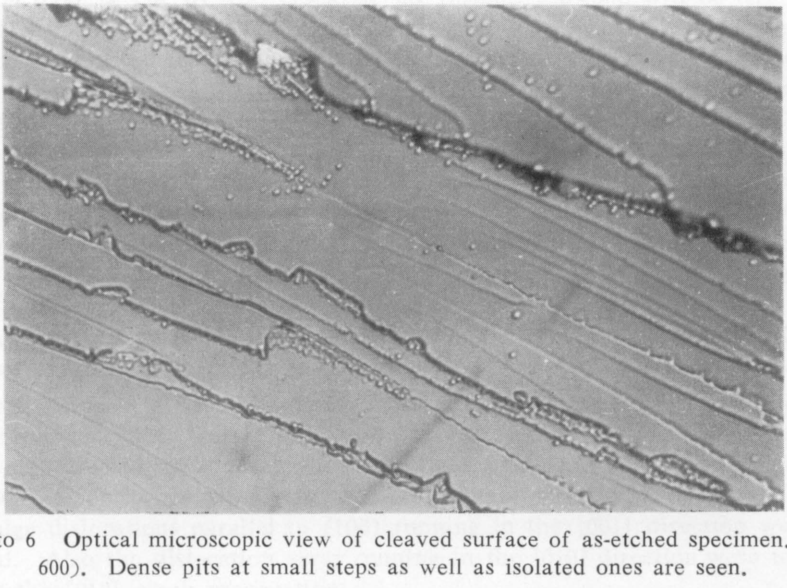

Photo 6 Optical microscopic view of cleaved surface of as-etched specimen. (× 600). Dense pits at small steps as well as isolated ones are seen.

(*Facing* p. 26)

shows the nucleation of fresh dislocations.

4. 2. Mechanism of nucleation of dislocations during cleavage

The mechanism of the nucleation of dislocations in MgO is presumably the same as that proposed by Burns *et al*,[12,13] in LiF single crystals. Among the possible, slip systems effective ones, on which a large stress concentration around the crack tip will result in the formation of dislocation loops, will be examined. Six slip systems, in the case of (100) cleaved plane, of {110} ⟨1$\bar{1}$0⟩ are shown in Fig. 4. If dislocation loops were induced on 90° bands as (011) [0$\bar{1}$1] in Fig. 4(a), they must have the [0$\bar{1}$1] Burgers vectors parallel to cleaved (001) plane. During the cleavage, however, slip planes perpendicular to cleaved plane can not be active, so that dislocations with Burgers vectors parallel to cleaved surface can not be nucleated. There is no possibility in this case that the dislocation loops like Fig. 4(a) are induced. Actually, no nucleation of long screw dislocations was observed in this experiments. Then in our experimental arrangement, active slip planes are of 45° bands. Fig. 4(b) shows (110) [$\bar{1}$10] and (1$\bar{1}$0) [$\bar{1}\bar{1}$0] and Fig. 4(c) (101) [$\bar{1}$01] and (10$\bar{1}$) [$\bar{1}$0$\bar{1}$].

In both case, the dislocation which appears on the cleavage surface is a screw type and the one dragged through crystal is an edge type. When a crack proceeds in the [010] direction as shown in Fig. 5(a), a small dislocation loop having the Burgers vector of $\boldsymbol{b}=a_0/2[\bar{1}01]$ will be created on (101) slip plane by stress concentration. If the speed of the crack is so high that created dislocation loop is cut by the crack at an instant, the loop will be left on the slip plane as a small half-dislocation loop. In this case, small atomic steps will possibly remain.[13] If the cleavage crack moves at a comparative speed with that of the dislocation, the resulting dislocation loop is also small. Even then half-dislocation loops are created in this state, they will be aged by the imaging force and escape out of the surface, leaving rather high steps. When the speed of cleavage is sufficiently lower than that of dislocations, the crack propagation will associate a heavy dragging of the created dislocation loops. As a result, long edge dislocations will be nucleated and left behind at some distance from the cleavage surface as shown in Fig. 5(c). The dislocation nucleated by this dragging is parallel to the cleavage surface. Its penetration depth was found to be nearly equal to the radius r of the original dislocation loop. r is known to depend upon the stress at the crack tip.

In the region A crack propagation was probably hindered by the large step. The river lines show that the direction of crack propagation in this part was [011] as a whole. It is decomposed into two components, [001] and [010]. For the [001] crack propagation, the two slip planes, (110) and (1$\bar{1}$0), are active and edge dislocations parallel to (100) running in the [001] direction were nucleated. Also the dislocation array running in the [010] direction were nucleated for the [010] crack propagation.

Above discussions are supported by the results : few cleavage steps were observed in the regions where dislocations were detected, while steps about

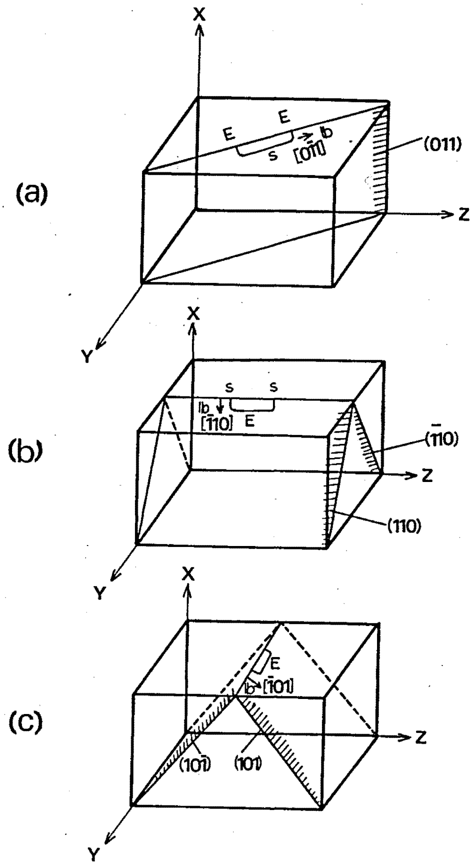

Fig. 4 Possible dislocation half loops in the slip planes.
(a) is 90° band which can not act during cleavage.
(b) and (c) are 45° band.

thousands Å in height were observed in the regions where no dislocations were detected. And at these steps, small and shallow etch pits were concentrated as shown in Photo 6. This means that, in this part, the crack propagated faster than in the part where dislocation array was observed by X-ray topography. And this is the case shown in Fig. 5(b). The area of fracture surface where fresh dislocations were detected is optically smooth. Similar results have been previously obtained by observing the fracture surface of iron single crystals, as reported by one of the authors.[24]

The ductile-brittle transition temperature of LiF is about 300°C. So cleavage at room temperature is reasonably accompanied by a considerable amount of plastic work, *i.e.*, a crack hesitates during the cleavage and forms a deformation zone increasing plastic work. In the case of MgO, the transition temperature

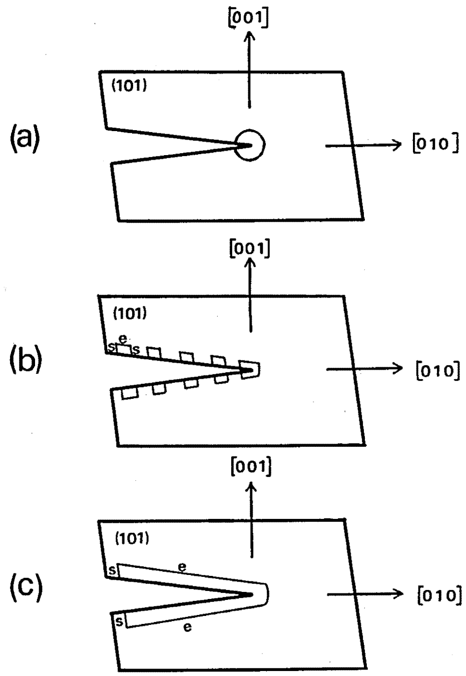

Fig. 5 Schematic diagram of the mechanism of dislocation loops nucleation along slip trace.
(a) nucleation at the crack tip.
(b) crack speed is rather fast and small dislocation loops are nucleated.
(c) crack speed is rather low and long edge dislocations are dragged through crystal.

is high and the propagation rate of crack is extremely high in the cleavage at room temperature. A large amount of plastic work cannot be expected during cleavage. The cause of the nucleation of dislocations will be attributed to the slowing down of cleavage at large steps.

4. 3. Stress field around the tip of the cleavage crack

The mechanism of dislocation nucleation in MgO crystals does not seem to differ from that in LiF as the lowering of cleavage speed has an important role in both cases. Some simple estimations will be given on the present results based on the theory of LiF cleavage developed by Burns *et al.*[11,12] If the crack velocity is much lower than the velocity of sound, the resolved shear stress, τ_c, that may act on dislocations in the (110) plane with a Burgers vector of $a_0/2$ $[1\bar{1}0]$ around the tip of an (100) plane crack moving in the [010] direction has been calculated with the help of a formula due to Sneddon[25] for the stresses around a crack and the Peach-Koehler equation.[26]

$$\tau_c = \frac{P_0 C^{1/2}}{(2r)^{1/2}} \frac{1}{2} \left\{ (1-2\nu)\cos\frac{\phi}{2} - \frac{1}{4}\cos\frac{5\phi}{2} \right\}, \tag{1}$$

where P_0 is an effective pressure inside the crack, C half the crack length, r the magnitude of the radius vector from the tip of crack to any position in the slip plane, ν Poisson's ratio and ϕ the angle between r and the crack propagation direction.

A necessary condition for crack propagation is that the energy released by the elastic-strain field as the crack expands be sufficient to create the new cleavage surface. Applied as the Griffith criterion,[27] this yields for P_0 of eq. (1) :

$$P_0 = \left(\frac{2E\gamma_0}{\pi(1-\nu^2)C} \right)^{1/2}, \tag{2}$$

where γ_0 is intrinsic surface energy and E Young's modulus. To calculate the value of τ_c, ϕ can be represented by an effective angle $\bar{\phi}$ which can be deduced from experiments. Then,

$$\tau_c \cong \frac{1}{2} \left(\frac{E\gamma_0}{\pi(1-\nu^2)} \right)^{1/2} \frac{1}{r^{1/2}} \times \left\{ (1-2\nu)\cos\frac{\bar{\phi}}{2} - \frac{1}{4}\cos\frac{5\bar{\phi}}{2} \right\} \equiv \frac{B}{r^{1/2}}. \tag{3}$$

We use a value of 45° for $\bar{\phi}$ on the basis of an optical examination in ionic crystal,[28] though Burns *et al.*[12] took 53° for $\bar{\phi}$ in LiF in their original study. Value of B will be now estimated by using various quantities on MgO. The principal moduli of MgO are $C_{11}=28.9\times10^{11}$dyn/cm^2 and $C_{12}=8.7\times10^{11}$dyn/cm^2 by Durand[29] and Chung[30] and its Young's modulus 24.817×10^{11} dyn/cm^2. Then $\nu=0.2313$. By Westwood and Goldheim,[31] the intrinsic surface energy at 20°C is $\gamma_0=1150\pm80$ ergs/cm^2. Then the value of B is given by $B=2.9\times10^6$dyn/cm. This value agrees with that of LiF.

Effective shear stress τ applied to the dislocation is given by

$$\tau = \frac{B}{r^{1/2}} - \frac{Gb}{\pi r}, \tag{4}$$

where G is shear modulus and b the magnitude of Burgers vector. Equation (4) has maximum stress $\tau_{max}=\pi B^2/4Gb$ at $r=4G^2b^2/\pi^2B^2$.

4. 4. Dislocation velocity

For further steps, the dislocation velocity in MgO have to be given. But this is not experimentally given, though measurements of dislocation velocities in many other substances were made. Among these substances,

$$v = v_D(\tau/D)^m \tag{5}$$

explains the experimental results well. D and m are constants depending on a nature and a state of substances, and v_D is generally chosen to be 1cm/sec. In this case D is the stress for dislocation to move with the velocity of 1cm/sec.

$$v = v_0 \exp(-A/\tau) \tag{6}$$

can also explain the experimental results.[32] v_0 and A are constants independent to τ.

In general, eq. (6) shows better fit over a wide range than eq. (5). In this paper as a wide range of dislocation velocities, from very high velocity to low one, are treated, we assume eq. (6) to hold in the case of MgO crystals. In eq. (6), v_0 is the maximum velocity of dislocation which is assumed to be 30% of the sound velocity v_t.[32] The value of A can be evaluated from the following considerations. When the speed of the cleavage crack reaches approximately 1% of v_t, the plastic work takes place suddenly.[12,13] At that time, the velocity of dislocations is a little faster than that of crack propagation. Then a value of A is determined by the condition that the velocity of dislocations at τ_{max} is equal to 1% of v_t. The value of A thus determined is 4.836×10^8 dyn/cm^2 or 4.928 kg/mm^2. Fig. 6 shows $v-\tau$ curves of many substances,[33] which have been measured, and the calculated curves of MgO. In comparison, the value A of MgO is roughly same as that of NaCl,[34] LiF[35] and Ge[36] and seems reasonable.

When $v-\tau$ curves are analyzed by eq. (5), the value of m is 3.5 on LiF and MgO and 2.7 on NaCl for $v>10^2$, and for $v<10^2$ it is 16.7 on LiF and

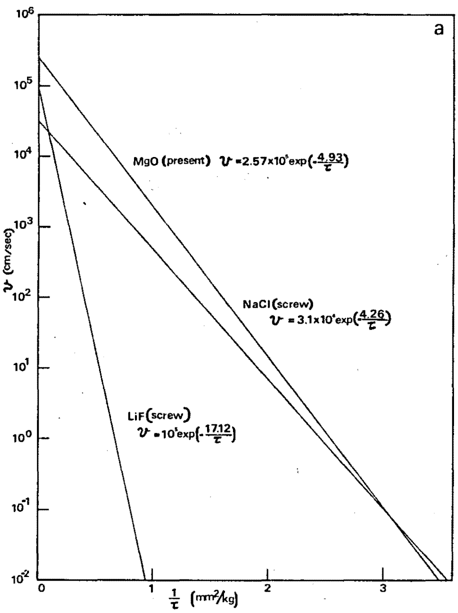

Fig. 6 Dislocation velocities as a function of stress of various substances. The curve of MgO was calculated by eq. (6) and the other were experimentally measured by many workers.[33] (a) plotted as logarithm of velocity versus reciprocal stress. Eq. (6) of ionic crystals was also shown.

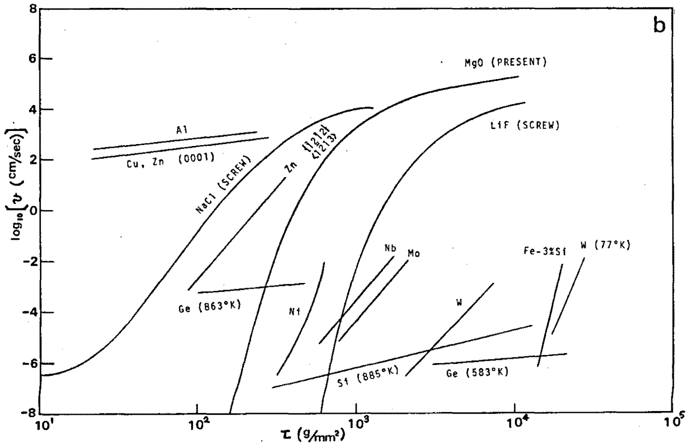

Fig. 6 (b)

(b) plotted as logarithm of velocity versus stress. Data indicated with no temperature were measured at room temperature.

MgO and 8 on NaCl. This shows a good agreement between LiF and MgO.

4. 5. Discussions on various quantities

Combining eqs.(4) and (5) yields the form

$$v=v_0 \exp\left(\frac{-A}{\frac{B}{r^{1/2}}-\frac{Gb}{\pi r}}\right), \tag{7}$$

where the dislocation speed v nearly equal to the speed of cleavage and r nearly equal to the depth of a dislocation penetrated in a crystal from the surface. The relation between v and r is shown in Fig. 7. When v is smaller than $v_{\max}$, for example $v=10^3$ cm/sec, the radius of the smallest dislocation loop is 0.4μm and that of the largest is 7 μm. The smaller one escapes out from surface because of the imaging force and the only the larger one is dragged. This radius of dislocation is considered to equal to depth r_d from the surface. In this figure the observed dislocation depth, $r_d=10\mu$m, corresponds to the crack velocity, $v_d \sim 5\times10^2$ cm/sec.

The work W due to the motion of dislocations, is determined by the following equation.[13]

$$W=(bA)\left[\sqrt{2}\, r_d L/(\ln v_0/v_d)\right], \tag{8}$$

where L is the crack length, taken as equal to 0.1cm. Then we obtain $W \cong 3 \times 10^{-4}$ erg. Effective surface energy is given by[13]

$$\gamma=\gamma_0+\frac{\alpha W}{L}, \tag{9}$$

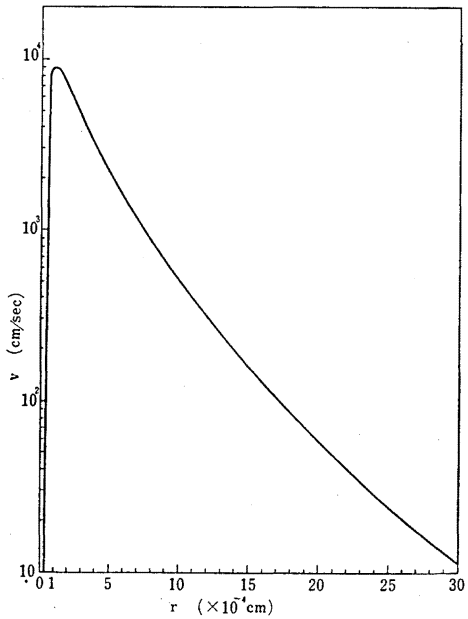

Fig. 7 Relation between the crack velocity and the penetration depth of fresh dislocation calculated by eq. (7).

where α is the fresh dislocation density. The second term of right hand of eq. (9) is the increment in the effective surface energy due to the plastic work. This increment estimated here is several per-cent of intrinsic surface energy and is much smaller than that of LiF.

It is concluded that generally in the cleavage of MgO crystal the contribution of plastic works to its effective surface energy is very slight at room temperature. However, the increment of the surface energy caused by the change of the crack speed during cleavage can be sometimes too great to be neglected. This is possibly the reason of the discrepancy between the present results and the theory of fracture in ideal crystals proposed by Tyson *et al*,[16] concerning the amount of plastic deformation.

References

1) Kelly, A., *Strong Solids*, (Clarendon Press, Oxford, 1966).
2) Hulse, C. O., Formation and Strength of Magnesia Whiskers, J. Amer. Ceramic Soc., Vol. 44, 1961, p. 572.
3) Stokes, R. J., Dislocation Sources and the Strength of Magnesium Oxide Single Crystals, Trans. AIME, Vol. 224, 1962, p. 1227.
4) Day, R. B. and Stokes, R. J., Mechanical Behavior of Magnesium Oxide at High Temperature, J. Amer. Ceram. Soc., Vol. 47, 1964, p. 493.
5) Argon, A. S. and Orowan, E., Crack Nucleation in MgO Single Crystals, Phil.

Mag., Vol. 9, 1964, p. 1023.
6) Lange, F. F., Transgranular Fracture Studies on Magnesium Oxide Bicrystals, Phil. Mag., Vol. 16, 1967, p. 761.
7) Lange, F. F. and Lambe, K. A. D., Interaction between a Crack Front and Cleavage Steps, Phil. Mag., Vol. 18, 1968, p. 129.
8) Gilman, J. J., Knudsen, C. and Walsh, W. P., Cleavage Cracks and Dislocation in LiF Crystals, J. appl. Phys., Vol. 29, 1958, p. 601.
9) Gilman, J. J., Creation of Cleavage Steps by Dislocation, Trans. AIME, Vol. 212, 1958, p. 310.
10) Forty, A. J., The Generation of Dislocations during Cleavage, Proc. Roy. Soc. (London), Ser. A, Vol. 242, 1957, p. 392.
11) Washburn, J., Gorum, A. E. and Paker, E. R., Cause of Cleavage Fractures in Ductile Materials, Trans. AIME, Vol. 215, 1959, p. 230.
12) Burns, S. J. and Webb, W. W., Plastic Deformation during Cleavage of LiF, Trans. AIME, Vol. 236, 1966, p. 1165.
13) Burns, S. J. and Webb, W. W., Fracture Surface Energies and Dislocation Process during Dynamical Cleavage of LiF, I. Theory and II. Experiments, J. appl. Phys., Vol. 41, 1970, p. 2078 and p. 2086.
14) Forwood, C. T. and Lawn, B. R., Plastic Deformation Patterns on Cleavage Surfaces of Lithium Fluoride, Phil. Mag., Vol. 13, 1966. p. 595.
15) Tyson, W. R., Theoretical Strength of Perfect Crystals, Phil. Mag., Vol. 14, 1966, p. 925.
16) Kelly, A., Tyson, W. R. and Cottrell, A. H., Ductile and Brittle Crystals, Phil. Mag., Vol. 15, 1967. p. 567.
17) Futagami, K., Study on Crystal Lattice Defect by the X-Ray Diffraction Topography, Rep. Res. Inst. Appl. Mech., Vol. XVII, No. 57, 1969, p. 49.
18) Futagami, K. X-Ray Studies on the Sub-Grain Boundaries of LiF Single Crystals by the Limited Projection Topography, Japan. J. appl. Phys., Vol. 6, No. 12, 1967, p. 1381.
19) Lang, A. R., Applications of 'Limited projection topographs' and 'Direct beam topographs' in diffraction topography, Brit. J. appl. Phys., Vol. 14, 1963, p. 904.
20) Friedel, J., "*Fracture*" (Wiley Inc., New York, 1959) Propagation of Cracks and Work Hardening, p. 498.
21) Tetelman, A. S., "*Fracture of Solids*" (Intersc., New York, 1959), The Plastic Deformation at the Tip of a Moving Crack, p. 461.
22) Gilman, J. J., Nucleation of Dislocation loops by Cracks in Crystal, Trans. AIME, Vol. 209, 1957, p. 449.
23) Kitajima, K., On the Mechanism of Cleavage Fracture of Crystals, Proc. 1st Intern. Conf. Fracture, Vol. 2, 1966, Sendai, p. 647; Fundamental Studies on the Plastic Deformation and Brittle Fracture of Iron [in Japanese], Bull. Res. Inst. Appl. Mech. No. 19, 1962, p. 1.
24) Kitajima, K and Futagami, K., Fractographic Studies on the Cleavage Fracture of Single Crystals of Iron, Amer. Soc. Test. Mat., Vol. STP 453, 1969, p. 33.
25) Peach, M and Koehler, J. S., The Forces Exerted on Dislocations and the Stress Fields Produced by Them, Phys. Rev., Ser. 2. Vol. 80, 1950, p. 436.
26) Sneddon, I. N., The Distribution of Stress in the Neighbourhood of a Crack in an Elastic Solid, Proc. Roy. Soc. (London) Ser. A, Vol. 187, 1946, p. 229.
27) Griffith, A. A., The Phenomena of Rupture and Flow in Solid, Phil. Trans. Roy. Soc., Vol. A221, 1921, p. 163.
28) Shaskol'skaya, M. P., Yen-wen, Wang and Kushu-chao, Generation of Disloca-

tions in the Propagation and Coalescence of Cracks in Ionic Crystals, Soviet Phys. Crystallography, Vol. 6, No. 4, 1962, p. 483. (Kristallografiya, Vol. 6, No. 4, 1961, p. 605)

29) Durand, Milo A., The Temperature Variation of the Elastic Moduli of NaCl, KCl and MgO, Phys. Rev., Vol. 50, 1936, p. 449.

30) Chung, Dae-Hyun, Elastic Moduli of Single Crystal and Polycrystalline MgO, Phil. Mag., Vol. 8, 1963, p. 833.

31) Westwood, A. R. C. and Goldheim, D. L., Cleavage Surface Energy of {100} Magnesium Oxide, J. appl. Phys., Vol. 34, No. 11, 1963, p. 3335.

32) Gilman, J. J., Dislocation Mobility in Crystals, J. appl. Phys., Vol. 36, No. 10, 1965, p. 3195.

33) For example; Sumino, K., "Teni no Undo to Kessho no Henkei 2" [in Japanese], Bull. of the Japan Institute of Metals, Vol. 10, No. 11, 1971, pp. 759-767.

34) Gutmanas, E. U., Nadgornyl, E. M. and Stepanov, A. V., Dislocation Movement in Sodium Chloride Crystals, Soviet Phys. -Solid State, Vol. 5, 1963,p. 743.

35) Johnston, W. G. and Gilman, J. J., Dislocation Velocities, Dislocation Densities, and Plastic Flow in Lithium Fluoride Crystals, J. appl. Phys., Vol. 30, 1959, p. 129.

36) Schäfer, S., Messung von Versetzungsgeschwindigkeiten in Germanium, Phys. Stat. Solidi, Vol. 19, 1967, p. 297.

(Received November 30, 1972)